

Density reduction and beam scattering and straggling in gas targets: influence on radionuclide yield and recovery

S.-J. Heselius

Accelerator Laboratory, Abo Akademi,
Turku, Finland

Abstract

This article reviews the literature on density reduction in gas targets used for accelerator production of radionuclides. Basic studies of this matter in connection to nuclear physics research are discussed. The role of beam scattering and straggling in gas targets is briefly considered. The bibliography contains the most relevant and useful references on density reduction and beam scattering and straggling with respect to radionuclide production from gas targets.

Density Reduction in Gas Targets

In measurements of the differential cross-sections for neutron production via the $T(d,n)^4\text{He}$ reaction in tritium gas targets Bame and Perry <1> noticed a loss in the yield of neutrons from the target with increasing beam current. This loss was attributed to a reduction in the density of tritium atoms in the region of the target through which the beam passed. A linear decrease in the neutron yield was observed with increasing beam current. The gas-heating effect was measured for 0.25 - 7.25 MeV deuterons on tritium. The work was carried out at Los Alamos Scientific Laboratory and was reported in 1957.

In 1961, Robertson, White and Erdman <2> studied density reduction effects in oxygen and deuterium gas targets at 0.5 and 1 atm pressure, respectively. In their article "Beam Heating in Gas Targets", published in the same year, they stated that the effect of beam heating of the target gas must be taken into account in accurate cross-section measurements. The study was carried out at the University of British Columbia, Vancouver, Canada. A 900 keV proton beam of 0.1 - 1.2 μA beam current was used. A diagram of the gas target assembly used in the study is shown in Fig. 1. The energy of the protons entering the gas was fixed and determined by the accelerator voltage. The energy loss (ΔE) of the protons in the target gas is proportional to the atomic stopping cross section and the number of atoms per cm^2 . The proton energy leaving the gas was set by the requirement that the gamma-ray yield from 873 keV resonance of the $^{19}\text{F}(p,\alpha,\gamma)$ -reaction due to protons striking a thin calcium fluoride-target was a maximum. The constancy of the density in the beam volume was ensured by maintaining ΔE constant. The pressure $P(I)$ required to maintain the given target thickness, i.e. the density ρ , constant was measured as the beam current I was varied. By a linear extrapolation to the $P(I)$ values to zero beam current, a pressure $P(O)$ was obtained. The

ratio $P(I)/P(0)$ was plotted as a function of beam current. The density P in the beam volume is given by

$$p = [P(I)/P(0)][T/T_{\text{eff}}]p(0)$$

where $p(0)$ is the gas density at zero beam current (temperature T and pressure $P(0)$), $P(I)$ is the target pressure at beam I and T_{eff} is the average temperature in the beam strike. Since the target gas density in the beam volume was constant the pressure ratio directly gave an estimate of the average temperature of the gas in the volume traversed by the beam by multiplying the ratio with the temperature T for zero beam current. Thus the average temperature in the beam strike:

$$T_{\text{eff}} = [P(I)/P(0)]T$$

Eleven years later, in 1972, McDaniels, Bergqvist, Drake and Martin <3> published an article "Beam Heating in Gas Targets". They studied the reduction in density of the gas due to beam heating by measuring the flux of neutrons emitted from a proton irradiated tritium gas target as a function of the beam current. The correction from the change in density of molecules in gas targets as a function of the beam current was investigated using both a pulsed beam and a dc beam. For the pulsed beam a plastic neutron detector was mounted at 110° to the incident beam. Measurements made with the dc beam utilized a proton recoil counter telescope consisting of a CH_2 radiator foil and a NaI(Tl) scintillator. Foil in and out run were made to establish the net telescope counts for subtraction of the background due to photon radiation. McDaniels et al. stated that the dominant physical mechanism responsible for the decrease in density of the target gas atoms was heating of the gas. No dependence on pulsing of the beam was found. Within the measurement error both the dc and pulsed measurements had the same dependence on the effective temperature of the gas cell. The measurements were carried out with a 12 MeV proton beam of the Los Alamos Scientific Laboratory tandem Van De Graaff accelerator. The target pressure was 2.6 atm.

In 1980 Görres and co-workers <4> reported that for a constant target pressure the geometrical location of the narrow resonance at $E(p) = 278$ keV for the $^{14}\text{N}(p,\gamma)^{15}\text{O}$ reaction moves along the beam axis when the beam intensity is varied. They concluded that the density of the gas target along the beam axis depends on both the energy loss per unit length and the ion beam current, i.e. the power dissipated in the gas. They used a 350 keV accelerator at the University of Münster. The accelerator provided beam currents up to 300 μA . The investigation was carried out in the pressure range 0.25 – 10 Torr.

All the above reviewed observations concerning density reduction in the beam strike of a gas target were connected to nuclear physics measurements. A common observation among researchers concerned with production of radionuclides from gas targets has been that there is a lack of proportionality between the radionuclide yield and the particle beam current at a fixed particle energy incident on the target. Oselka, Gindler and Friedman <5> have reported that the radionuclide yield was not proportional to the beam current or gas pressure in the production of ^{81}Rb from ^{82}Kr . They inserted a conductivity probe into the deuteron beam volume of a nitrogen gas target. The gas conductivity was measured as a function of the beam current on the target at 1–30 psi absolute pressure. Their investigation showed that for all beam currents greater than 1 μA the number of ionized molecules in the beam volume is essentially independent of the

pressure and reaches a plateau between 5 and 10 μA beam current. They suggested that a high temperature in the beam was one of the reasons why gas molecules are forced out of the beam volume as the beam intensity on the target is increased.

The non-linear relationship between radionuclide yield and particle beam current at fixed incident particle energy on a gas target has been observed by several research groups. In 1979 Ruth and Wolf discussed the density reduction in an article published in the IEEE Transactions on Nuclear Science <6>. The Brookhaven group also reported their observations obtained with the $^{18}\text{F}-\text{F}_2$ target system in an article in the Journal of Nuclear Medicine (Ref. 7, Casella et al., 1980). They stated that the increase in temperature caused by the beam results in a reduction in gas density and thus decreases the number of target nuclei in the beam volume. This results in a lower radionuclide production rate.

In the 3rd Symposium on Radiopharmaceutical Chemistry in St. Louis (1980), Wieland and co-workers <8> reported an experimental target developed for studies of beam penetration in gas targets. A diagram of this target is shown in Figure 2. The target was equipped with a thin aluminum exit window followed by a 1.3 mm thick gas cavity and an electrically insulated water-cooled aluminum beam stop. Charged particles penetrating the exit window produce over a voltage gap (300 V) an ion current which is measured with an electro-meter to estimate the beam penetration. Ion collection curves for 10.7 MeV deuterons incident on a Ne-gas target are shown in Figure 3. The voltage gap current is shown as a function of the neon pressure at different beam currents on the target. The break points where the gap current rises sharply represent the pressure insuring thick target conditions since the 1.1 MeV deuteron energy required to penetrate the 3.45 mg/cm^2 thick aluminum exit window matches the $^{20}\text{Ne}(\text{d},\alpha)^{18}\text{F}$ threshold <8>.

A more extensive study of charged particle penetration in gas targets using the voltage gap method was reported by Wieland, Schlyer and Wolf in 1984 <9>. In this work an alternative method for determining the target gas pressure at which the beam penetrates to the end of the target was discovered. It was observed that the pressure ratio (beam on vs beam off) goes through a maximum at this condition, as can be seen in Figure 4. At pressures where the beam is entering the end flange of the target, the energy deposition in the gas is small and the pressure ratio is low. At high pressures when the beam is stopping early in the target the heat transfer is good and the pressure ratio again is low. The maximum ratio is an indicator of the lowest pressure giving thick target conditions. A good correlation between the results of the pressure ratio method and the exit window method can be seen in Figure 4. Both the pressure ratio method and the exit window method have been widely used by several groups working with optimization of gas target performance for radiopharmaceutical preparation <10>.

At the Abo Akademi Accelerator Laboratory (Turku, Finland) optical methods have been used in order to study the behaviour of particle beams in gas targets <11-16>. Direct photography of the light emitted by target gas atoms in the beam has been used to study the shape and penetration of particle beams in gas targets as well as the scattering of the beam in different windows and in the target gas. The particle beam was photographed through a glass window on an experimental target chamber <11,16> using a remote-controlled camera. The following parameters were varied:

- Target gas volume and pressure
- target chamber shape
- beam collimations

- target chamber entrance window materials and thicknesses
- particle energy and beam intensity
- temperature of the target cooling medium

A reduction of the target-gas density in the beam volume can clearly be seen in the form of an increased particle penetration range as a function of the beam current on the target. At high beam currents an asymmetric shape of the beam is observed when the beam is viewed horizontally. The asymmetric beam shape indicates an increased particle penetration range as a function of vertical position in the beam. The asymmetric density reduction is due to an upward thermal transport of the heated gas in the target chamber. The density is increasingly reduced as one moves up in the beam due to the thermal upward stream. For high beam currents ($>5 \mu\text{A}$) the least dense region in the gas target is above the beam. When the beam is viewed vertically, no asymmetry is observed. A typical horizontal view is seen in Figure 5, which shows Ar bombarded with alpha-particles.

With an interferometric arrangement <11> using a He-Ne laser and a target chamber equipped with two opposite glass windows, interferograms of the target gas have been recorded showing variations in the refractive index of the gas caused by the particle beam. Figure 6 shows an interferogram recorded of Argon at 675 kPa initial pressure bombarded with 17.7 MeV alpha-particles of 4.0 μA beam current.

Estimates of the temperature distribution in the target can be made from the interferograms <11,12>. In Figure 6 a vertical dashed line has been drawn. By measuring the position of the interference fringes along the dashed line in the vertical plane from the bottom of the top of the chamber, one can make a cross-sectional plot of the variation in optical path-length in relation to the conditions at the bottom. At each fringe a constant increment in the ordinate is made corresponding to $\lambda/2$ in the optical pathlength. The obtained diagrams of fringe number against vertical fringe position for Ar at 675 kPa initial pressure bombarded with 17.7 MeV alpha-particles of 1-6 μA beam current are shown in Figure 7. As can be seen, an almost linear change in fringe number (and temperature) takes place in the beam region showing an upward increasing density reduction in the beam.

The strong upward thermal transport of the heated gas from the beam region observed in the interferometric studies was verified by inserting a stainless steel liner into a production target chamber <13>. The chamber was filled with ^{nat}Kr and irradiated with 18 MeV protons. After the irradiation the liner was removed and cut into pieces in order to measure the distribution of amounts of ^{81}Rb and ^{82m}Rb on the stainless steel liner. The results of the measurements <13> support the strong upward gravitational transport observed with interferometry.

The Abo Akademi group continued their optical studies related to gas targetry with the development of a spectroscopic method by which the density reduction and temperature increase in a pressurized gas target bombarded with high energy particles can be quantified by studying the widths of the atomic emission lines from the ion-beam excited target medium <14,15>. The method was applied in a study of the widths of some emission lines from a deuteron-beam excited Ne-gas target. It was observed that the spectral line width is a linear function of the pressure within the pressure region studied (20-500 kPa). A reduction in the line width was observed with increasing beam current. This was interpreted as being due to the density reduction caused by the particle beam. As a result of the study a method was obtained to measure the temperature

at any position in the beam volume.

Beam Scattering and Straggling

When a parallel beam of heavy charged particles passes through a medium, the particles are scattered and the beam diameter is gradually expanding with increasing depth, mainly due to Coulomb-force interactions between the incident particles and the nuclei of the medium. This expansion is due partly to the cumulative effect of many small particle deflections, and partly to large single-event deflections of relatively few of the particles. The first type of process is called multiple scattering, while the second is referred to as single scattering. For most practical applications multiple scattering through small angles predominates over single scattering.

Multiple scattering plays an important role in the design of gas targets since the angular spread of a charged particle beam emerging from a target window and undergoing further scattering in the target gas will cause a loss of production capability if the target diameter is such that the scattered beam strikes the walls of the target chamber. Numerical calculations can be carried out for the multiple scattering of charged particles in order to evaluate whether the scattered beam could reach the target walls. Several methods permitting a rapid evaluation of the multiple scattering angular distributions for charged particles in scattering media can be found in the literature. Useful methods are those by Snyder and Scott <17> and Marion and Zimmermann <18>. A rapid evaluation of the multiple scattering angular distribution with an error of less than 10 % can be made from the graph worked out by Millburn and Schechter <19>. The graph gives the root mean square angle of multiple scattering for protons, deuterons and alphas which have traversed a fraction X/R_0 of their mean range R_0 in the target.

Particle beam scattering can also experimentally be evaluated by activation of foils placed in the target chamber at different distances from the beam entrance window. The distribution of radioactivity induced in the foils can be studied by autoradiography or more accurately by cutting the foils into small pieces and measuring the radioactivity in the pieces with a Ge(Li)-detector. Good agreement between experiment and theory has been achieved using these procedures <9,10>. This is also true for the method using direct photography of the particle beam through a glass window on the target chamber <11>. An experimental study on scattering of charged particles (p,d,³He and alpha) in metal foils commonly used as target windows (Al, Fe, Cu, Ni and Havar) has recently been carried out by Schlyer <20>. The results of this study also show a good agreement with theoretical predictions.

Charged particles lose kinetic energy to an absorbing medium primarily in small discrete amounts as they undergo a multitude of microscopic interactions such as atomic ionization and excitation, elastic nuclear collisions and charge exchange with the atoms of the medium. Since these are statistical or stochastic processes, an initially monoenergetic beam of charged particles will acquire an energy spread after passing through an absorber. There will therefore exist a statistical distribution of the energy loss by the charged particles which have travelled identical path-lengths in the stopping material. The width of this energy distribution is a measure of energy straggling which varies with the distance along the particle track.

Charged particles are consequently subject to range straggling and path-length straggling defined as the fluctuation in range and path-length, respectively, for individual particles of the same initial energy. The same stochastic factors that lead to energy straggling at a given penetration distance thus result in slightly different total path-length for each particle. The charged particles will not have the same number of interactions and the energy transfer in each interaction varies. For charged particles such as protons or alphas, the range straggling amounts to a few per cent of the mean range <21>. Multiple scattering from the atomic potential will make the range straggling distribution slightly wider than the path-length straggling distribution <22>. The range straggling is most conveniently described in terms of the full width, 2σ , at half maximum of the Gaussian distribution of ranges for particles of different energies (Figure 8). The percentage range straggling, $100 \times 2\sigma / R_0$ for protons, deuterons and alphas for energies between 10 MeV and 1000 MeV can rapidly be evaluated from the graphs of Millburn and Schechter <19>. Values for straggling about the mean path-length for protons can be found in the extensive proton range-energy tables made by Janni <22,23>.

Yield and Recovery versus Beam Current and Total Charge

If the initial target pressure is lower than the pressure required for thick target conditions for the particle energy used the radionuclide yield may be significantly lower than the expected thick target yield and does not increase linearly with the beam intensity. While the initial pressure still represents a thick target, an intense particle beam may reduce the target density to such an extent that the target is no longer sufficiently thick to stop the beam or to degrade the incident beam energy to the practical threshold energy of the nuclear reaction. Scattering of the beam by the target chamber entrance windows and by the target gas as well as reduction of the target gas density seriously affect the location of the energy deposition in the target causing a loss in the production capability of the particle beam. In order to obtain yields in agreement with those of a thick target and linearity between yield and beam intensity one must carefully optimize the target system with respect to both scattering and density reduction <10,16>. One should be convinced that the target still represents the thickness required for the beam current to be used in the irradiation. Because the extent of density reduction in the target depends on the volume of the target system <16,24> data concerning target length and required target pressure should not be directly transferred from one target system to another unless these systems are comparable with respect to volume and shape.

A linear dependence between the yield of ^{11}C and the proton beam intensity on a nitrogen gas target optimized with respect to density reduction and beam scattering has been reported by Vandewalle and Vandecasteele <10>. Their yields of $^{11}\text{CO}_2$ from a nitrogen gas target are in good agreement with experimentally determined thick target yields for the $^{14}\text{N}(p,\alpha)^{11}\text{C}$ reaction and with the thick target yields earlier reported <25>. Clark and Buckingham <26> have also reported a linear dependence between the recovery of ^{15}O and the beam current in the production of ^{15}O from a nitrogen gas target with a deuteron beam.

Mulders <27> investigated the dependence of beam current and initial target pressure on the production rate of ^{81}Rb and $^{82\text{m}}\text{Rb}$ from natural krypton gas bombarded

with protons. The bombarding energy and energy decrease in the target were chosen in an energy region (20 – 22 MeV) where the cross-section from the production of ^{81}Rb and $^{82\text{m}}\text{Rb}$ from Krypton could be considered constant <27>. This means that changes in the production rate are only due to changes in the local gas density when the beam current on the target is increased. Thus, it was possible to make a direct statement about the average gas density at the position of the proton beam. The production rates of ^{81}Rb and $^{82\text{m}}\text{Rb}$ at different beam currents were measured and normalized to the rates at 1 μA beam current on the target. A decrease of about 15 % was observed in the production rate for a beam current of 16 μA and a gas pressure of 400 kPa (target chamber length 10 cm). Mulders stated that the density of the gas at the position of the proton beam was reduced by 10–15 % at a beam current of 16 μA . The beam current density was 12 $\mu\text{A}/\text{cm}^2$.

Casella et al. <7> studied the effect of beam current (also called dose rate) on the recovery of ^{18}F from a deuteron irradiated Ne-gas target containing 0.1 % F_2 . The study indicated that the recovery remained constant (>90 % of theoretical) for 1–10 μA beam current on the target, but began to decrease at higher beam currents so that at 15 μA the recovery was cirka 83 % of the theoretical value. The measurements were made at a constant total charge (also called total dose) on the target. The recovery of ^{18}F from the target was also studied as a function of the total charge given to the target. It was found that the total charge delivered to the target had a dramatic effect on the recovery of the ^{18}F at high charges. A decrease in recovery of ^{18}F was observed with increasing charge to the target. Although one would expect higher yields at a lower beam current the added irradiation time required to obtain an equivalent production of ^{18}F was found to be prohibitive <7>. Similar results have also been obtained by other groups.

Conclusions

The results of the studies concerning changes in density reduction of pressurized gas targets bombarded with high energy particles are consistent with an explanation of thermal heating as the mechanism of target gas density reduction <9>.

Multiple scattering in the target window and further in the target gas should be taken into account in the design of target chambers. Scattering of the beam by the target chamber entrance windows and by the target gas as well as reduction of the target gas density seriously affect the location of the energy deposition in the target, causing a loss in the production capability of the particle beam. Numerical calculations according to multiple scattering theories for charged particles can be carried out in order to evaluate whether the beam scattered in the target entrance foil can reach the target chamber walls. Experimental studies of particle beam scattering in foils and gases have shown good agreement with theoretical predictions.

The most important part of the target system with respect to beam scattering is the entrance foil. A thin entrance foil made of a material with a low atomic number and a low density should be used in order to minimize the beam scattering. However, in general a high target pressure is required and therefore the entrance foil must have a high

mechanical strength also at high temperatures. Of special interest are the beam foils used for the new generation of low-energy "medical" accelerators. Thin windows should be used in order to minimize the energy loss of the particles in the foils.

Radionuclides are frequently produced from thin gas targets via high yield (p,xn)- and (d,xn)-reactions. Measuring the flux of fast neutrons produced in the target during irradiation gives direct information about the density reduction in thin gas targets and reliably predicts the radioactivity buildup in the target <28>. This method can be used as a measure of the effective beam current on the target.

A linear dependence between radionuclide yield and beam intensity can be obtained using a target system optimized with respect to density reduction and beam scattering. Because the extent of density reduction in the target depends on the volume of the target system, data concerning target length and required target pressure should not be directly transferred from one target system to another unless these systems are comparable with respect to volume and shape. The density reduction in each target system should be evaluated separately.

The density reduction in a gas target also depends on focusing of the beam. A narrow focused beam causes a stronger density reduction in the beam path than a defocused beam of the same intensity. Beam or target motion is to be preferred whenever possible to obtain a more diffuse energy deposition in the target gas and the target entrance window. Other important parameters in connection to density reduction are target pressure and target cooling. A high target pressure gives a better heat transfer in the gas and a low target wall temperature also lowers the average temperature in the beam strike. These and other aspects concerning density reduction are further discussed in Ref. <9>.

Acknowledgements

The author is grateful to Prof. Marten Brenner for criticism of the manuscript and to Mrs Karin von Schalien for her kind help with typing the manuscript.

References

1. S.J. Bame, Jr. and J.E. Perry, Jr., T(d,n)⁴He Reaction, Phys. Rev. 107 (1957) 1616-1620
2. L.P. Robertson, B.L. White and K.L. Erdman, Beam Heating Effects in Gas Targets, Rev. Sci. Instr. 32 (1961) 1405.
3. D.K. McDaniels, I. Bergqvist, D. Drake and J.T. Martin, Beam Heating in Gas Targets, Nucl. Instr. and Meth. 99 (1972) 77-80.

4. J. Gorres, K.U. Kettner, H. Krawinkel and C. Rolfs, The Influences of Intense Ion Beams on Gas Target Densities, *Nucl. Instr. and Meth.* 177 (1980) 295–303.
5. M. Oselka, J.E. Gindler and A.M. Friedman, Non-Linear Behaviour of Gas Targets for Isotope Production, *Int. J. Appl. Radiat. Isot.* 28 (1977) 804–805.
6. T.J. Ruth and A.P. Wolf, "Small" Accelerator, Radionuclide and Radiopharmaceutical Production, *IEEE Trans. Nucl. Sci.* NS-26 (1979) 1710–1712.
7. V. Casella, T. Ido, A.P. Wolf, J.S. Fowler, R.R. MacGregor and T.J. Ruth, Anhydrous F-18 Labelled Elemental Fluorine for Radiopharmaceutical Preparations, *J. Nucl. Med.* 21 (1980) 750–757.
8. B.W. Wieland, D.J. Schlyer, T.J. Ruth and A.P. Wolf, Deuteron Beam Penetration in a Neon Gas Target for Producing Fluorine-18, *J. Labelled Comp. Radiopharm.* 18 (1981) 27–29.
9. B.W. Wieland, D.J. Schlyer and A.P. Wolf, Charged Particle Penetration in Gas Targets Designed for Accelerator Production of Radionuclides Used in Nuclear Medicine, *Int. J. Appl. Radiat. Isot.* 35 (1984) 387–396.
10. T. Vandewalle and C. Vandecasteele, Optimisation of the Production of $^{11}\text{CO}_2$ by Proton Irradiation of Nitrogen Gas, *Int. J. Appl. Radiat. Isot.* 34 (1983) 1459–1464.
11. S-J. Heselius, P. Lindblom and O. Solin, Optical Studies of the Influence of an Intense Ion Beam on High Pressure Gas Targets, *Int. J. Appl. Radiat. Isot.* 33 (1982) 653–659.
12. S-J. Heselius, P. Lindblom and O. Solin, Interferometric Studies of the Influence of an Intense Ion Beam on High Pressure Gas Targets, *J. Labelled Comp. Radiopharm.* 19 (1982) 1343–1345.
13. O. Solin, S-J. Heselius, P. Lindblom and P. Manngard, Production of ^{81}Rb from Kr – A Target Study, *J. Labelled Comp. Radiopharm.* 21 (1984) 1275–1277.
14. S-J. Heselius, P. Lindblom, E.M. Nyman and O. Solin, Studies of Emissionline Profiles from Ion-excited Neon Gas Targets, *Int. J. Appl. Radiat. Isot.* 35 (1984) 977–980.
15. O. Solin, S-J. Heselius, P. Lindblom and E.M. Nyman, Density Reduction and Temperature Mapping in a Ne-Gas Target, *J. Labelled Comp. Radiopharm.* 21 (1984) 1278–1280.
16. S-J. Heselius, P. Malmberg, O. Solin and B. Langstrom, Production of Carbon-11 with Respect to Specific Radioactivity – A Target Study, *J. Labelled Comp. Radiopharm.* 21 (1984) 1254–1256.
17. H.S. Snyder and W.T. Scott, Multiple Scattering of Fast Charged Particles, *Phys. Rev.* 76 (1949) 220–225.
18. J.B. Marion and B.A. Zimmermann, Multiple Scattering of Charged Particles, *Nucl. Instr. and Meth.* 51 (1967) 93–101.
19. G.P. Millburn and L. Schechter, Graphs of RMS Multiple Scattering Angle and Range Straggling for High Energy Charged Particles, Research Report UCRL-2234 (University of California, Radiation Laboratory, Berkeley, California, 1953).
20. D.J. Schlyer, manuscript in preparation.
21. G.F. Knoll, *Radiation Detection and Measurements* (John Wiley & Sons, Inc., New York, Chichester, Brisbane and Toronto, 1979) pp. 44–49.
22. J.F. Janni, Proton-Range Energy Tables, 1 keV–10GeV, *Atomic Data and Nuclear Data Tables* 27 (1982) Nos 2/3 and 4/5.

23. J.F. Janni, Calculations of Energy Loss, Range, Pathlength, Straggling, Multiple Scattering and the Probability of Inelastic Nuclear Collisions for 0.1 to 1000 MeV Protons, US Air Force Weapons Laboratory, Technical Report No. AFWL-TR-65-150, New Mexico (1966).
24. S-J. Heselius, P. Malmberg, O. Solin and B. Langstrom, Studies of Proton Beam Penetration in Nitrogen Gas Targets with Respect to the Production of Carbon-11 of High Specific Radioactivity, manuscript in preparation.
25. G.T. Bida, T.J. Ruth and A.P. Wolf, Experimentally Determined Thick Target Yields for the $^{14}\text{N}(p,\alpha)^{11}\text{C}$ Reaction, *Radiochim. Acta* 27 (1980) 181-185.
26. J.C. Clark and P.D. Buckingham, Short-lived Radioactive Gases for Clinical Use, Butterworth & Co. Ltd., London and Boston (1975) p. 132.
27. J.J.L. Mulders, Yield Curves and Beam Current Dependent Production Rates of Rb Radioisotopes Produced by Protons on a Krypton Gas Target, *Int. J. Appl. Radiat. Isot.* 35 (1984) 475-480.
28. R.J. Nickles, Target Telemetry for Medical Radionuclide Production, *Bull. Am. Phys. Soc.* 29 (1984) 1072.

Figure Captions

- Fig. 1. Gas target arrangement for study of beam heating effects. From Ref. 2.
- Fig. 2. Scheme of target for study of charged particle penetration of gases by voltage gap method. From Ref. 9.
- Fig. 3. Ion collection curves for 10.7 MeV deuterons incident on neon gas target in a 10.3 cm long target chamber. Voltage gap current as a function of target pressure is shown for various values of constant beam current. Curve (a) represents background current with 300 V across the gas cavity, curve (b) is background current with no voltage. From Ref. 9.
- Fig. 4. Comparison of methods for determination of pressure required to stop 10.7 MeV proton beam incident on nitrogen gas in a 10.3 cm long target chamber for $5 \mu\text{A}$ (dashed curves) and $10 \mu\text{A}$ (solid curves) beam current. From Ref. 9.
- Fig. 5. Horizontal view of Ar at 675 kPa initial pressure bombarded with 17.7 MeV alpha-particles of $6.0 \mu\text{A}$ beam current. Beam entrance from the right. From Ref. 11.
- Fig. 6. Recorded Interferogram of Ar at 675 kPa initial pressure, bombarded with 17.7 MeV alpha-particles of $4.0 \mu\text{A}$ beam current. Beam entrance from the right. The region with the largest optical path-length difference is shaded. From Ref. 11.
- Fig. 7. Fringe number and estimated temperature as a function of vertical position in an Ar target at 675 kPa initial pressure bombarded with 17.7 MeV alpha-particles of $1.0\text{--}6.0 \mu\text{A}$ beam current. The measuring position is marked in Fig. 6. From Ref. 12.
- Fig. 8. Illustration of the relationship between average path-length, mean range and path-length straggling. From Ref. 22.

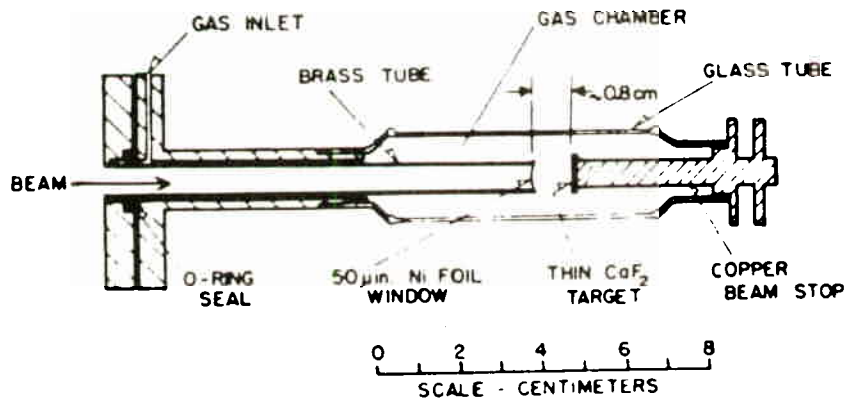


FIG. 1

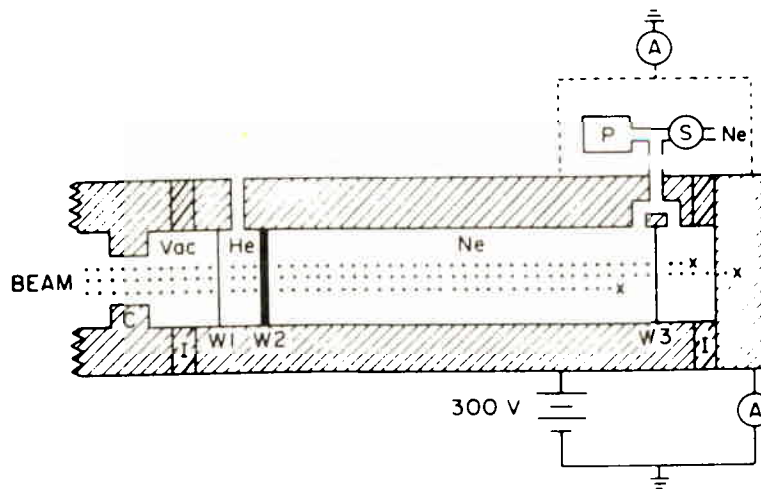


FIG. 2

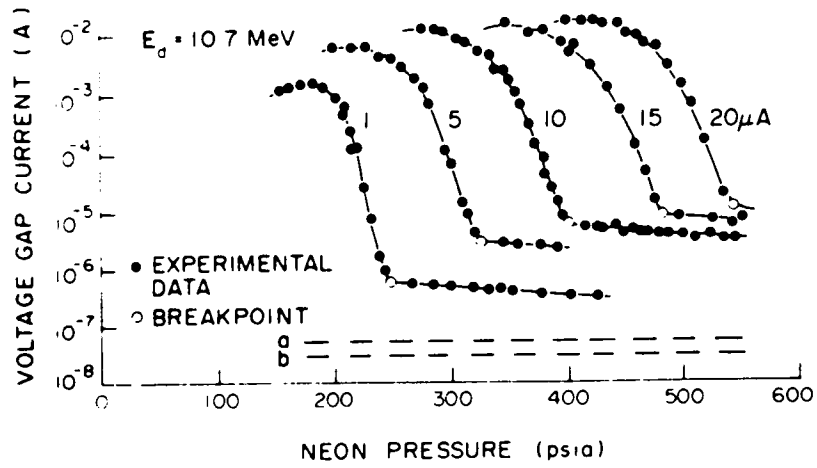


FIG. 3

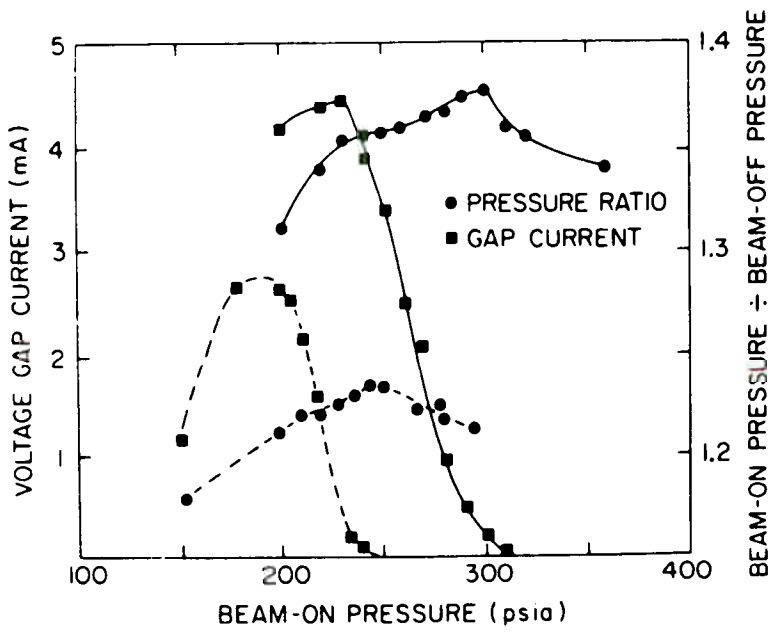


FIG. 4

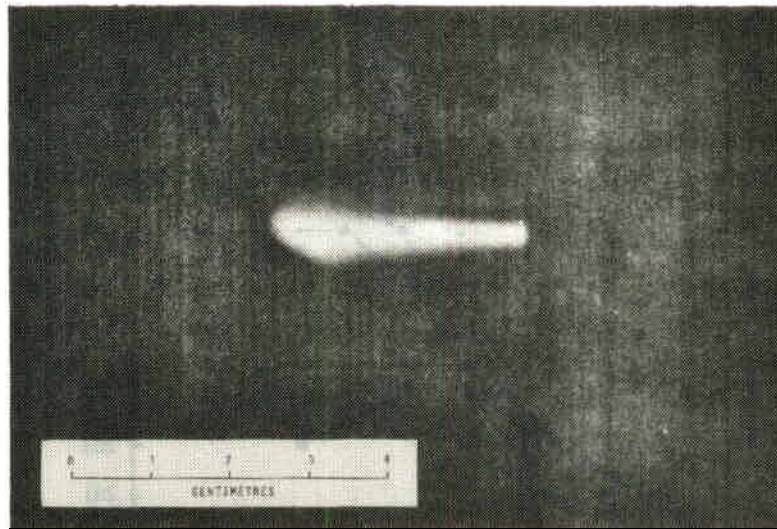


FIG. 5

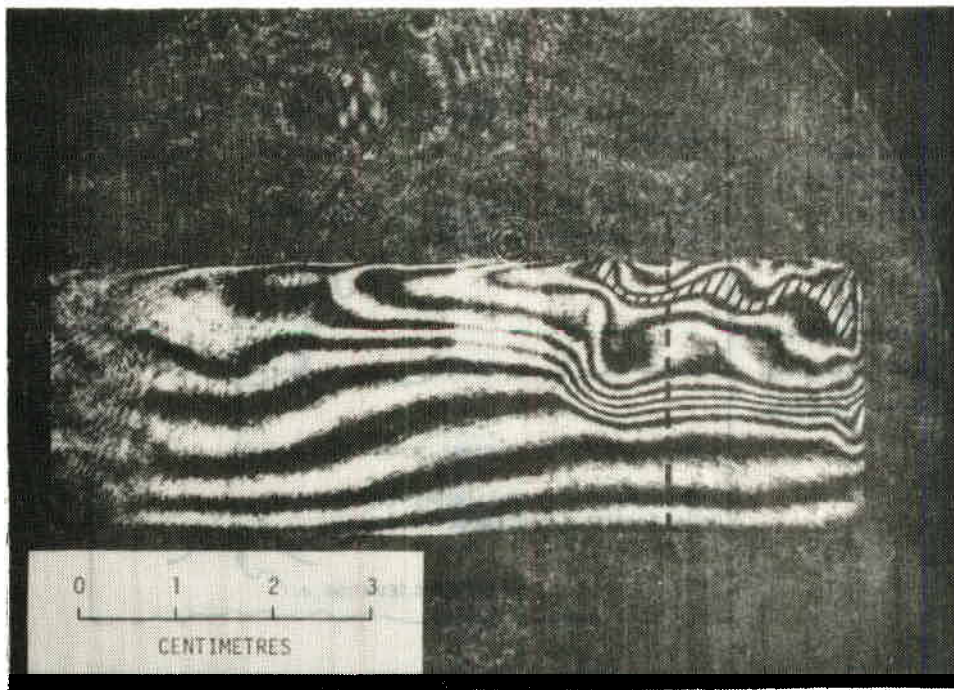


FIG. 6

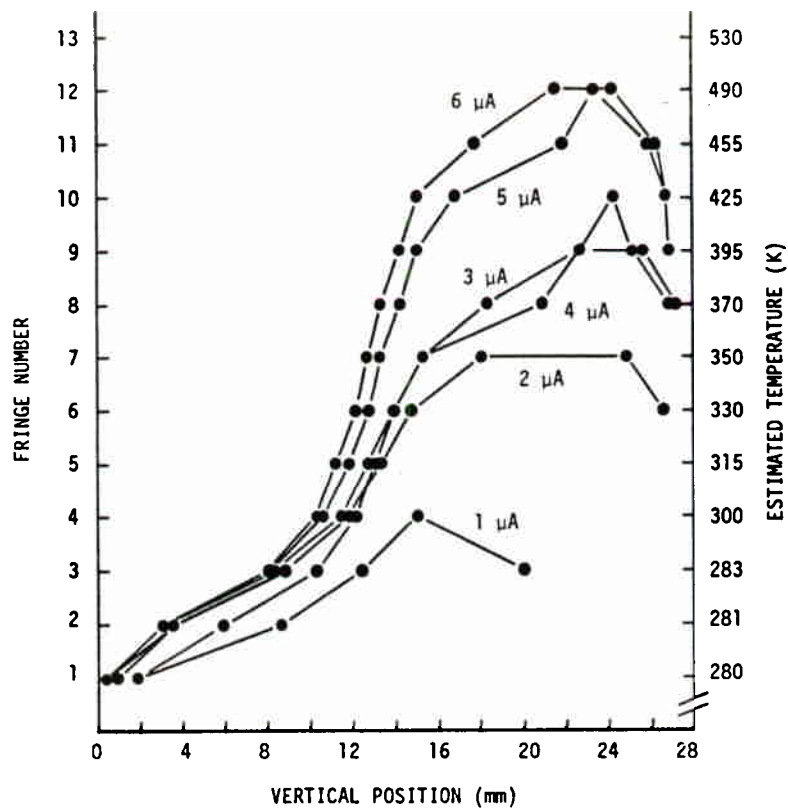


FIG. 7

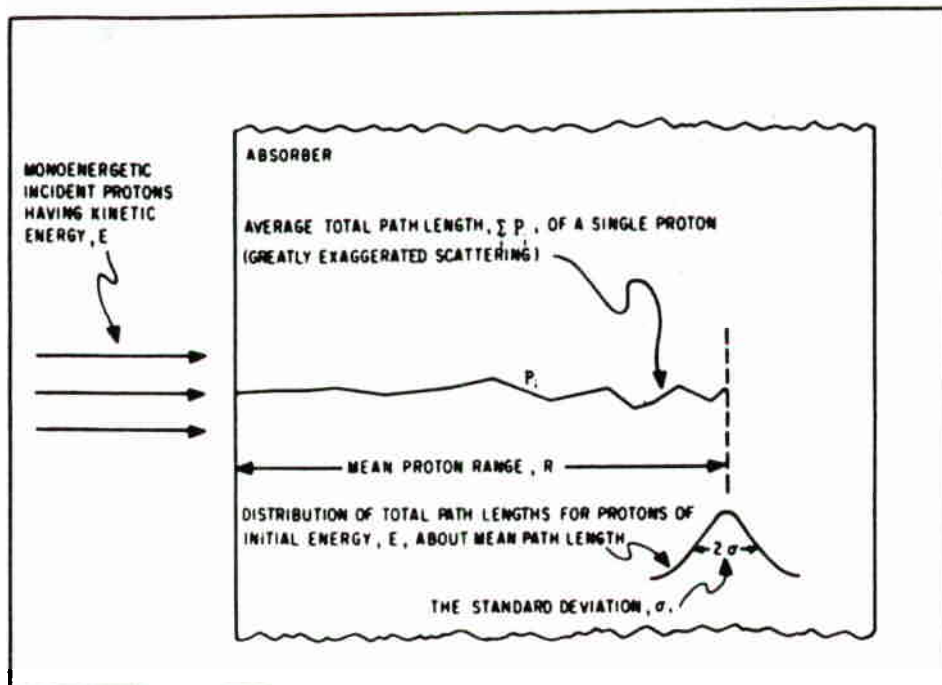


FIG. 8